Cancer Immunology, Immunotherapy (2023) 72:409–425
https://doi.org/10.1007/s00262-022-03238-w

ORIGINAL ARTICLE

Anti-mesothelin CAR-T immunotherapy in patients with ovarian cancer

Jiannan Chen[1] · Jianhua Hu[2] · Lili Gu[1] · Feng Ji[1] · Fan Zhang[1] · Miaomiao Zhang[1] · Jun Li[3] · Zhengliang Chen[3] · Longwei Jiang[2] · Yan Zhang[2] · Ruifang Shi[2] · Lihua Ma[2] · Shaochang Jia[2] · Ying Zhang[4] · Qi Zhang[5] · Junqing Liang[6] · Shunyu Yao[7] · Zhigang Hu[1] · Zhigang Guo[1]

Received: 1 December 2021 / Accepted: 6 June 2022 / Published online: 4 August 2022

Abstract

Recently, chimeric antigen receptor T cell (CAR-T) therapy has received increasing attention as an adoptive cellular immunotherapy that targets tumors. However, numerous challenges remain for the effective use of CAR-T to treat solid tumors, including ovarian cancer, which is an aggressive and metastatic cancer with a poor therapeutic response. We screened for an effective anti-MSLN single-chain Fv antibody with comparable binding activity and non-off-target properties using human phage display library. A second-generation of anti-MSLN CAR was designed and generated. We demonstrated the efficacy of our anti-MSLN CAR-T cells for ovarian cancer treatment in an in vitro experiment to kill ovarian tumor cell lines. The anti-MSLN CAR-T cells impeded MSLN-positive tumor growth concomitant with a significant increase in cytokine levels compared with the control. Then, we demonstrated the efficacy of anti-MSLN CAR-T cells in an in vivo experiment against ovarian cancer cell-derived xenografts. Furthermore, we herein report three cases with ovarian cancer who were treated with autologous anti-MSLN CAR-T cells and evaluate the safety and effectiveness of adoptive cell therapy. In this investigator-initiated clinical trials, no patients experienced cytokine release syndrome or neurological symptoms over 2 grads. Disease stabilized in two patients, with progression-free survival times of 5.8 and 4.6 months. Transient CAR expression was detected in patient blood after infusion each time. The tumor partially subsided, and the patient's condition was relieved. In conclusion, this work proves the efficacy of the anti-MSLN CAR-T treatment strategy in ovarian cancer and provides preliminary data for the development of further clinical trials.

Keywords CAR-T · Mesothelin · Immunotherapy · Ovarian cancer · Investigator-initiated clinical trial

Abbreviations

CDX	Cell-derived xenografts
CRS	Cytokine release syndrome
CT	Computed tomography
DLT	Dose-limiting toxicity
ELISA	Enzyme-linked immunosorbent assay
FDA	Food and Drug Administration
H&E	Hematoxylin and eosin
IARC	International Agency for Research on Cancer

Jiannan Chen, Jianhua Hu and Lili Gu have equally contributed to this work.

✉ Zhigang Hu
huzg_2000@126.com

✉ Zhigang Guo
guo@njnu.edu.cn

[1] Jiangsu Key Laboratory for Molecular and Medical Biotechnology, College of Life Sciences, Nanjing Normal University, Nanjing 210023, China

[2] Department of Biotherapy, Jinling Hospital of Nanjing University School of Medicine, Nanjing 210002, China

[3] Nanjing Blue Shield Biotechnology Co., Ltd., Nanjing 210023, China

[4] Department of Pathology, Jinling Hospital of Nanjing University School of Medicine, Nanjing 210002, China

[5] Center of Interventional Radiology and Vascular Surgery, Department of Radiology, Zhongda Hospital, Medical School, Southeast University, Nanjing 210009, China

[6] Inner Mongolia Autonomous Region Cancer Hospital, Hohhot 010010, China

[7] Baylor University, 1311 S 5th St, Waco, USA

NSCLC	Non-small cell lung cancer
PBMC	Peripheral blood mononuclear cells
PET	Positron emission tomography
PR	Partial response
SD	Stable disease
WBC	White blood cell

Introduction

Ovarian cancer is one of the most malignant gynecological malignancies with multiple recurrences and a very high mortality rate [1]. According to data released by the International Agency for Research on Cancer (IARC), there were 310,000 new ovarian cancer patients worldwide in 2020, of who 210,000 died [2]. Currently, the treatment of ovarian cancer is still based on surgical resection, radiotherapy, chemotherapy, and targeted therapy. However, 55–75% of patients who experience remission after first-line treatment relapse within 2 years, which results in a 5-year survival rate of less than 40% [3, 4]. Many patients with advanced ovarian cancer often fail to eradicate tumor lesions following surgery, leading to tumor recurrence and progression [5, 6]. Therefore, it is crucial that new treatment methods be explored.

According to the clinical data reported so far, the overall therapeutic effect of immune checkpoint inhibitor monotherapy in ovarian cancer is unsatisfactory. Of the adoptive immune cell therapies, chimeric antigen receptor T cell (CAR-T) therapy has developed the fastest and has yielded significant positive results in the treatment of hematological diseases [7]. CAR-T cell therapy uses a type of T cell that is genetically engineered to produce artificial T cell receptors. CARs are recombinant receptors, usually composed of extracellular antigen recognition domains, which are derived from single-chain variable fragments (scFv) of antibodies, transmembrane domains that anchor in the cell's plasma membrane and cells that deliver T inner domain [8, 9]. The first-generation CARs contain an intracellular signal component, usually a CD3ζ chain, that recognizes the target antigen and activates T cells but only produces short-term proliferative activity and low levels of cytotoxicity [10]. The addition of another costimulatory molecule (CD28, 4-1BB, or OX40) enabled the second-generation CARs to maintain proliferation and release cytokines [11]. At the same time, additional clinical trial results demonstrated the durability and stability of second-generation CAR-Ts in the body [12]. Since the first CAR-T cell therapy was approved by the US Food and Drug Administration (FDA) in 2017, the CAR-T therapy has made great achievements in the treatment of hematoma[13]. Currently, four CAR-T therapies targeting CD19 for B-cell malignancies and two targeting BCMA for the treatment of relapsed or refractory multiple myeloma has been successfully marketed worldwide [14, 15]. However, no CAR-T cell therapy project for ovarian cancer has yet been approved by the FDA or analogous drug administrations in other countries. Most CAR-T research on ovarian cancer is still at the preclinical research stage, and the resultant CAR-T cell functions are still limited in treatment [16, 17].

The recognition of tumor cells by CAR-T cells is determined by tumor-associated antigens from the perspective of treatment strategies. Mesothelin (MSLN), a glycosylphosphatidylinositol-anchored membrane glycoprotein, is highly expressed in many malignancies, including mesothelioma, non-small cell lung cancer (NSCLC), pancreatic cancer, and ovarian cancer, but has a highly restricted expression in normal adult tissues, such as the mesothelial lining of the pleura, peritoneum, and pericardium [18, 19]. This expression pattern makes MSLN an attractive target antigen and has resulted in clinical trials for a variety of therapeutics [20]. To date, MSLN has been used as a target for CAR-T cells against solid cancers, including mesothelioma, lung cancer, breast cancer, and pancreatic cancer [21]. Numerous preclinical studies have evaluated the safety and effectiveness of MSLN-targeting CAR-T cell therapy [17, 22, 23].

Although CAR-T therapy has proved highly efficacious against hematological tumors, several challenges remain for CAR-T therapy in the treatment of solid tumors, including ovarian cancer. Here, we screened for novel, effective scFv sequences with which CAR-T cells are constructed and implemented these CAR-T cells in clinical studies on ovarian cancer patients. A human anti-MSLN CAR that exhibited strong cytokine secretion and cytotoxicity on ovarian cancer cells in vitro and in vivo was designed and constructed. Furthermore, we evaluated the safety and efficacy of the anti-MSLN CAR-T cells on patients with advanced MSLN-positive ovarian malignancies by administering autologous CAR-T cells. Our research shows that anti-MSLN CAR-T cells have strong antitumor activity against MSLN-positive ovarian cancer cells and provide a promising immunotherapeutic strategy for the treatment of ovarian cancer.

Materials and methods

Screening anti-MSLN scFv.

Three rounds of panning were performed in immune tubes coated with recombinant MSLN using a fully human scFv phage display library, which had been previously constructed in our lab. Briefly, for the panning, a MSLN-His tag protein, and a phage-displayed natural scFv nanobody library were utilized as starting materials. Streptavidin-containing magnetic beads were added to bind with the biotin-containing MSLN-his protein and then incubated with the scFv-antibody library. Next, unbound phages

were removed by washing five times with 0.05% (v/v) Tween-20/PBS and twice with PBS; bound phages were eluted with 300 μL of 0.2 M glycine hydrochloride (pH 2.2) and neutralized with 45 μL of 1 M Tris–HCl for use in subsequent panning rounds. Changing the MSLN-His tag protein coating volume and washing conditions for each panning (three times in total) successively removed weakly bound phages and retained as many strongly bound phages as possible.

After infection of the -E.coli TG1 Strain, the solid medium plate was coated, and the enriched clones obtained from the third round of panning with strong binding ability were monoclonalized. Then, the monoclonal culture supernatant was used for enzyme-linked immunosorbent assay (ELISA) screening, and the nucleic acid sequence of the single clone was determined. If the absorbance signal was three times greater than the absorbance obtained with the BSA control, then the phage-scFv clone was considered a positive clone. The signal peptide of secreted luciferase, the antigen-binding site of nanobody, and the coding sequence of human IgG2Fc and His tag were connected, and then the mammalian expression vector was constructed along with frame reading. HEK293F cells were transfected, and the supernatant was retained for antibody purification using rProtein A magarose beads (Smart-Lifescience). low cytometry was used to detect the binding ability of MSLN antigen and purified antibody to screen out sequences with high affinity. Then the antibodies were further co-incubated with targeted cells expressing different MSLN antigens to screen out highly specific antibody sequences.

Real-time binding kinetics analysis

The binding kinetics of G11 antibody against MSLN was analyzed by Bio-Layer Interferometry (BLI) according to the manufacturer's instruction. The kinetic constants including ka, kdis, and KD were analyzed by using ForteBio data analysis software ver. 7.1.

Construction of a basic second-generation of anti-MSLN CAR-T cell

The extracellular portion of the chimeric antigen receptor (CAR) molecule is typically generated from a monoclonal antibody against the target. The variable heavy (VH) and variable light (VL) chains, also known as the single chain variable fragment (scFv), from the antibody sequence are connected by a linker to form the antigen specific region of the CAR molecule. The hinge or spacer region anchors the scFv to the transmembrane region that traverses the cell membrane. Intracellularly, the costimulatory domain and CD3ζ chain signal once the scFv portion of the CAR recognizes and binds tumor antigen.

Cells and culture conditions

HEK293 (human embryonic kidney 293 cells), Hela (human cervical carcinoma cell line), Ovcar3 (human ovarian cancer cells), SKOV3 (human ovarian adenocarcinoma), Tov-21g (human ovarian clear cell carcinoma) and Huh7 (human liver cancer cells) cell lines were obtained from the American Type Culture Collection (ATCC). Peripheral blood mononuclear cells (PBMCs, TPCS#PB025C) of normal people were purchased from the miles-bio of Shanghai. The patient's PBMCs were provided by the partner hospital for scientific research. The HEK293 $^{MSLN+}$ was generated by transfecting the parental cell line with a lentiviral supernatant containing MSLN. Prior to the experiment, all cell lines were identified and validated, and routine tests were performed on mycoplasma. All cells are cultured in the recommended medium supplemented with FBS at 37 °C in an atmosphere of 5% carbon dioxide.

T cell isolation and retroviral transduction

PBMCs from healthy donors and ovarian cancer patients were isolated by Lymphoprep (Stemcell, Canada), and then T cells were isolated from the cells by negative selection using EasySep™ Human T Cell Isolation Kit (Stemcell, Canada). Then activated using anti-human CD3 and CD28 microspheres (Miltenyi, Germany) at a 3:1 bead to cell ratio on day 0. Purified T cells were cultured in 5% FBS X-VIVO Serum-free Hematopoietic Cell Medium (Lonza, Switzerland) supplemented with recombinant human IL-2 (300 IU/mL). Detection of the CAR-T cell positive rate and detection of cell phenotype was performed following lentivirus infection and continuous culture for 48 h after T cell isolation. Using anti-MSLN CAR-T cells, paired (from same donor) untransduced T cells, activated and cultured for equivalent time, served as control T cells or Mock CAR-Ts.

Retrovirus production and transduction of primary T cells

Transient transfection of 293 T cells with plasmids for MSLN-CAR constructs, RDF plasmid encoding the RD114 envelope, and PegPam3 plasmid encoding the MoMLV gag-pol was used to generate retroviral supernatants. T cells sorted in the previous step were resuspended with 100 μL of MSLN CAR-Ts lentivirus and inoculated in 96-well plates for 4 h to incubate. Then transferred cells to into 24-well

plates. After 48 h, cells were washed and replated in cultured in X-VIVO Serum-free Hematopoietic Cell Medium and maintained in incubators at 37 °C with 5% CO_2. In addition, replenished with fresh medium and IL-2 every 2 days.

Flow cytometry

The antibodies used in this study, including anti-CD3-FITC, CD4-PE, CD8-APC, CD45RA-PC7, CD62L-PB450, CD45RO-APC and CCR7-PE were purchased from BD (San Diego, CA), and monoclonal antibodies at 1:100 dilution. Anti-MSLN antibody was from R & D Systems. Isotype-matched control mAbs were applied in all the procedures. All FACS-related staining procedures were kept out of dark at room temperature. Cells were washed with washing buffer or 3 times after incubation for 30 min at 4 °C and then all samples were acquired on a CytoFLEX S (Beckman Coulter, Indianapolis, IN), and data were analyzed using Kaluza 2.1 Flow Analysis Software (Beckman Coulter Life Sciences).

Impedance-based kinetics cell lysis assay

Real-time impedance analysis of cell lysis kinetics was evaluated over 50 h. HEK293, Huh7, Hela, Ovcar3 and Skov3 cells were plated in a 96-well resistor bottom plate at 2.0×10^4 cells per well. After cultured for 24 h, effector T cells were added into the unit at different effector/target cell (E: T) ratios (8:1, 4:1, 2:1, and 1:1). Impedance was measured at 28 s intervals. The impedance-based cell index for each well and time point was normalized with the cell index before adding T or CAR-T cells. The kinetics of cell lysis was evaluated as the change in normalized cell index over time.

Mouse tumor models

Female B-NDG mice (6 weeks) were purchased from Biocytogen (Beijing). All procedures were conducted in conformity with guidelines of the National Institutes of Health and Institutional Animal Care and Use Committee. And the animal experiments were approved by the Nanjing Normal University Animal Faculty. Mice were maintained under specific pathogen-free conditions for 3 days, then an equal number of Ovcar3 cells (1×10^7/per mouse) were subcutaneously implanted on the right of the same B-NDG mice, respectively. On the 29th day, all mice were randomly divided into 5 groups ($n=6$/group) and different groups were treated with PBS, 1×10^7 Mock CAR-T cells and different doses of anti-MSLN CAR-T cells at one time (1×10^7, 3×10^6 and 1×10^6). Then we changed the administration method and doses of CAR-T cells in the next hela cell cdx animal model. Hela cells (1×10^7/per mouse) were subcutaneously implanted on the right of the same B-NDG mouse. On the 16th day, all mice were randomly divided into 5 groups (n = 10/group) and different groups were treated with PBS, 5×10^6 Mock CAR-T cells and lower different doses of anti-MSLN CAR-T cells (5×10^6, 2.5×10^6 and 1×10^6). 10%, 30%, 60% of the total dose was administered by tail vein injection for three consecutive days. In the Tov-21g model, we first subcutaneously inoculated B-NDG mice with 1×10^7 tumor cells. When the tumor volume grows to be large enough without extravasation, the tissue is removed under aseptic conditions and cut into tumor pieces with a volume of 3–4 mm^3 and inoculated into new NDG mice. Due to uneven tumor formation, only 12 were used for the experiment. We divided them into two groups and administered PBS and 1×10^7 CAR-T cells through the tail vein, respectively. Tumor growth was measured with caliper, and tumor volume was calculated using the formula volume = (length × width × width) × 0.5. Survival time was defined as the time when tumor volume reaches 1200 mm^3. Collect blood from mice before execution for blood routine and blood biochemical testing.

Immunohistochemistry (IHC)

Tissues were fixed with formalin and embedded in paraffin until further processing. Then 3-mm-thick sections were deparaffinized and treated with a heat-induced antigen IHC Tek epitope retrieval solution (IHC World) for 30 min. Slides were then blocked with tris-NaCl (TNB) blocking buffer (PerkinElmer) and stained with anti-human CD3ε antibody (Abcam, Grand Island, NY) or anti-human MSLN antibody (Abcam, Grand Island, NY) in the blocking solution overnight at 4 °C. Secondary antibodies were added after rinsing the section for 1 h at room temperature, and the results were visualized with a ChemMate Envision Detection Kit (DakoCytomation). Images were obtained using the 3DHISTECH Panoramic digital slide scanner and the associated CaseViewer software (3DHISTECH).

Measurement of cytokines

The Human IL-2, TNF-α, IFN-γ kit of the R&D Biological ELISA Development Kit were used to measure concentrations of culture supernatant and animal serum according to the manufacturer's instructions. Briefly, 2×10^4 cultured tumor cells seeded in 96-well plates and cultured for 24 h. Then cocultured with T cells, Mock CAR-T and MSLN CAR-T at an effector-to-target ratio of 1:1, 2:1, 4:1, 8:1. Cell culture supernatants were collected at 72 h, centrifuged, and frozen until the time of assay. Blood of mice and patients was left at room temperature for 20 min to clot and get serum by centrifugation. Each experiment was independently performed in triplicate.

Clinical trial design and specimen collection

Here, we report the results of an investigator-Initiated clinical study conducted in accordance with the principles of the Declaration of Helsinki to evaluate the safety and pharmacokinetic characteristics of MSLN CAR-T in humans and to perform preliminary exploration of its antitumor activity.

Patients who were screened for MSLN expression must have relapsed at least twice within 2 years, following the criteria described in the Guidelines for the Diagnosis and Treatment of Ovarian Malignant Tumors (2018 edition). Their MSLN expression status was determined via immunohistochemistry (IHC) staining of fresh tumor samples or archived samples collected at local laboratories within 6 months before enrollment. MSLN expression was evaluated using a 4-point scale, with 0 indicating no MSLN expression (< 1%); 1 +, weak expression (1-25%); 2 +, medium expression (25–50%); and 3 +, strong expression (> 50%). Patients were eligible if they were 18 years or older, had histologically confirmed positive expression of ovarian epithelial cells, were not amenable to potentially curative surgical resection, or had at least one prior chemotherapy regimen that included pemetrexed and cisplatin or carboplatin. Informed consent for specimen uses for research purposes was obtained from all patients.

Patients who met all screening criteria for obtaining peripheral blood mononuclear cells (PBMC) for the generation of autologous anti-MSLN CAR-T cells were pretreated with fludarabine 3–5 days before receiving intravenous anti-MSLN CAR-T cells. The treating physician was able to adjust the lymphodepletion regimen according to the patient's disease condition. Two subjects (patient 002 and patient 003) were determined to be unfit for lymphodepletion due to heavy tumor burden and extremely elevated carbohydrate antigen 125 (CA12-5).

After lymph depletion, the patients received a cycle of anti-MSLN CAR-T cells therapy under observation and were not discharged from the hospital until their absolute neutrophil count returned to the normal range. In our study, anti-MSLN CAR-T cells were administered from a starting split dose (1×10^6 CAR-positive cells/kg) and gradually increased until the final total dose of the split infusion was reached. The maximum dose would be de-escalated if there was a dose-limiting toxicity (DLT) related to the CAR-T treatment. The total dose was administered in three sequential split infusions over the treatment cycle. The proportion of cells in each batch of infusion is 10, 30, and 60% of the total cell dose. The volume of cell suspension in each infusion is 110 ml, and the infusion is completed within 30 min. In the absence of toxicity or disease progression, these patients could receive additional cycles of anti-MSLN CAR-T cells treatment.

Patient response and progression were evaluated by the researcher via computed tomography (CT) and positron emission tomography (PET) scans as well as physical examinations before each cycle of infusion. Following the Solid Tumor Response Evaluation Criteria (RECIST) Guidelines (Version 1.1) and before each cycle of administration, serum was collected from patients treated with anti-MSLN CAR-T cells for the detection of physiological and biochemical indicators. At the same time, each patient's CAR-T cell DNA copy number, cytokine levels, and tumor marker gene expression were monitored after CAR-T cell infusion. Special attention was given to CAR-T-related infusion reactions, such as neurotoxicity and CRS.

qRT-PCR analysis of MSLN CAR-T DNA copy numbers

Real-time fluorescent qPCR was applied to determine the MSLN CAR-T DNA copy numbers in PBMC of three patients. Genomic DNA was extracted from patient PBMCs using a QIAamp DNA Blood Mini Kit (QIAGEN) before and after CAR T-cell infusion. The forward primer 5′-ACC TGGTCGACAATCAACC-3′, reverse primer 5′-AAGCAG CGTATCCACATAGC-3′, and TaqMan probe 5′-FAM-CAA AATTTG TGAAAGATTGACTGGT-TAMRA-3′ were used in the qPCR assay.

Results

Screen of humanized anti-MSLN scFv

Increased MSLN expression has been associated with a poor prognosis for patients with ovarian cancer [22]. The Kaplan–Meier analysis revealed that higher MSLN expression was associated with poor prognosis in patients with ovarian cancer (Fig. S1A). CAR-T immunotherapy targeting MSLN may be an effective means for the treatment of ovarian cancer. To obtain humanized antibody sequences for the anti-MSLN CAR-T therapy of ovarian cancer, a human scFv phage-displayed library was constructed based on a phagemid pcDNA 3.4 vectors and used for three rounds of liquid-phase panning (Fig. 1A). MSLN-binding clones were clearly enriched in screening (Fig. 1B). A monoclonal phage ELISA was employed to verify that these 14 positive phage clones specifically interacted with the MSLN protein but not with the negative control protein BSA (Fig. 1C). Based on the screened scFv, 14 full-length antibodies were constructed by fusing the VH and VL with a modified human IgG1. Yields for all produced antibodies are listed in Table S1. Even at a concentration of 10 ug/mL, six clones, including MB2, did not

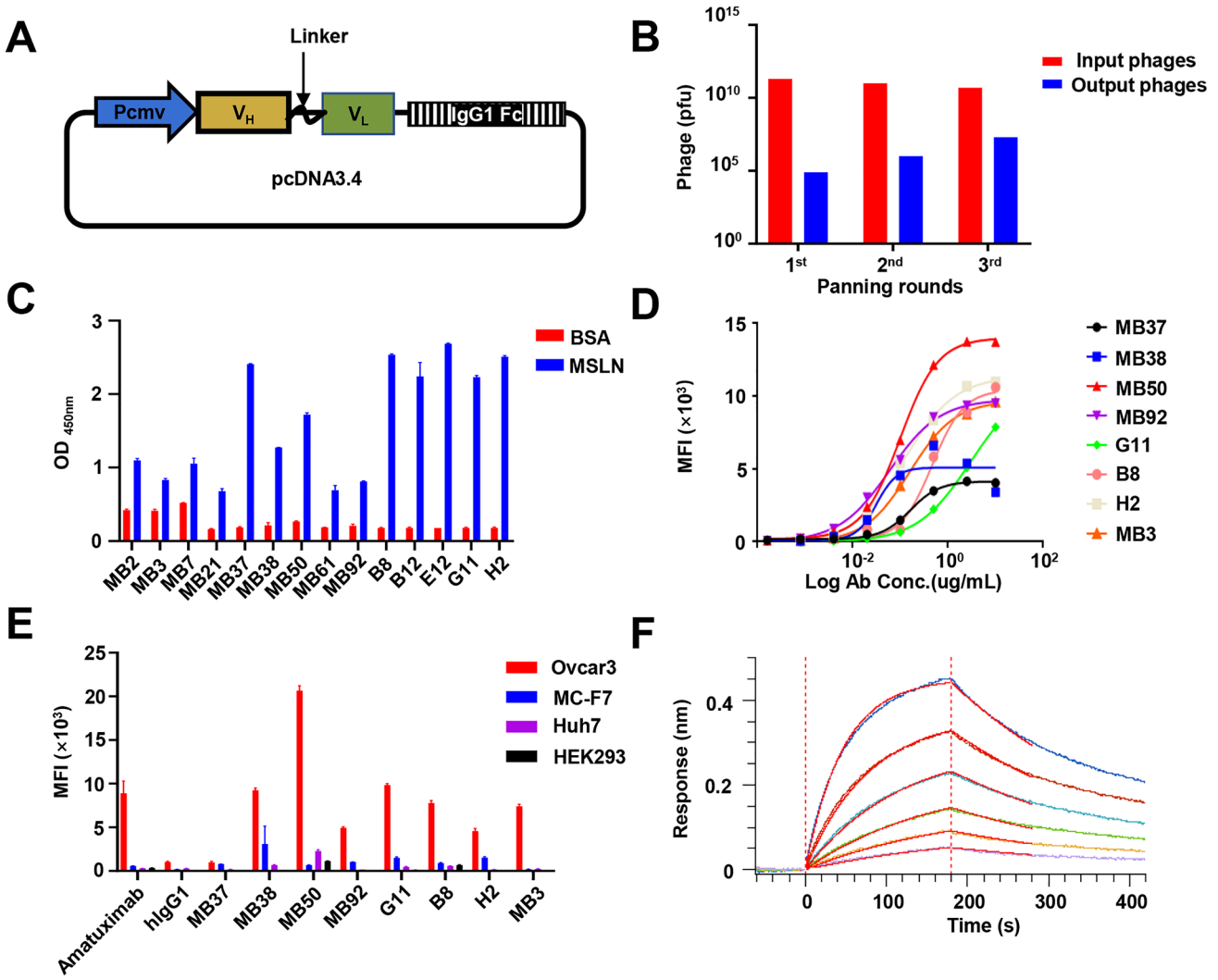

Fig. 1 Selection and expression of anti-MSLN scFv antibodies by phage display. **A** Scheme of phagemid vector pcDNA3.4 used for scFv display. **B** Enrichment of phage-displayed scFvs after each round of panning, and the output phages will be used for monoclonal screening. **C** Screening of positive clones bind to hMSLN by monoclonal phage ELISA. Each phage-displayed scFv was tested against hMSLN or BSA. **D** The antibody (ug/ml) with serial two-fold dilutions was mixed and incubated with tumor cells expressing MSLN. Characterization of six most potent binders by noncompetitive ELISA. SPR analysis of MSLN over a range of concentrations. **E** Detection of MSLN antibody specificity by flow cytometry. Ovcar3, a MSLN-positive cell line. MC-F7, Huh7 and HEK293 are MSLN-negative cell lines. **F** BLI sensor grams of G11cloned binding to biotin-labeled MSLN immobilized on SA chip

exhibit significant affinity for MSLN-positive tumor cells. Another eight antibodies with significant affinity were used for further detection (Fig. 1D). Antibodies which bound specifically to target cells and did not attack non-target cells were screened out via co-incubation with the MC-F7, Huh7, HEK293, and Ovcar3 cell lines. Four antibodies (MB37, MB38, MB50, and MB92) showed strong binding to MSLN-negative cells and could not be used as candidate antibodies for further CAR-T construction (Fig. 1E). Affinity is an important antigen-binding domain parameter as it fundamentally determines CAR-T cell functioning. Therefore, we tested the binding of G11 antibody to the MSLN antigen via surface plasmon resonance. The G11 antibody exhibited high affinity (KD = 2.35 nM) and a slow dissociation rate (Fig. 1F). Based on the above evaluation, we applied the G11 sequence to subsequent CAR-T studies owing to its comparable binding activity and non-off-target properties.

Construction and characterization of anti-MSLN CAR-T cells

We developed a second-generation, humanized CAR construct targeting MSLN, $MSLN^+$ CAR-T cells with the CD28 intracellular signal domain and CD3ζ intracellular signal domain (Fig. 2A). The G11 scFv of the MSLN antibody

was obtained via antibody screening, as described above. A mock CAR with the same intracellular stimulation signal except for the MSLN antibody scFv structure was designed to eliminate interfering intracellular signals. The transduction efficiency of $MSLN^+$ was stabilized at about 70.52% via FACS flow cytometry (Fig. 2B). Previous studies have demonstrated that T cell differentiation can significantly impact the outcome of immunotherapy. To ensure the quality and efficacy of the generated CAR-T cells, 12 days following lentiviral transduction, we determined the composition, and phenotypes of T cells, mock CAR-T and anti-MSLN CAR-T cells via flow cytometry analysis. The $CD4^+$/ $CD8^+$, CD45RA/CD62L and CD45RO/CCR7 ratio were not different among three groups cells as showed in Fig. 2C–E.

Anti-MSLN CAR-T cells repress cancer cells in vitro

Through flow cytometry, we detected the expression of the MSLN antigen in several cancer cell lines (Huh7, Hela, Skov3, and Ovcar3) and in HEK293 cells. The results indicated that MSLN was highly expressed in Ovcar3 and Hela cells but not in HEK293 cells and Huh7 cells (Fig. 3A). To determine the cytotoxicity, anti-MSLN CAR-T cells, or control T cells were co-cultured with the different cancer cell lines listed above. The results indicated that anti-MSLN-CAR-T cells efficiently poisoned MSLN-positive cell lines but not MSLN-negative (Huh7, HEK293) cells (Fig. 3B). Morphological analysis further verified the killing efficacy of anti-MSLN CAR-T cells on MSLN-positive cancer cells (Fig. 3C). On the contrary, the control T cells demonstrated low cell-killing ability. Consistently, significant amounts of interferon-γ (IFN-γ), interleukin-2 (IL-2), and tumor necrosis factor alpha (TNF-α) were detected in the co-culture medium containing anti-MSLN CAR-T cells and MSLN-positive cancer cell lines but not in that containing MSLN-negative cells (Fig. 3D). To confirm the specificity of anti-MSLN CAR-T cells in killing MSLN-positive tumor cells, we constructed an MSLN antigen-overexpression stable HEK293 cell line ($HEK293^{MSLN+}$) (Fig. 3E) and conducted in vitro killing experiments. Our data confirmed that anti-MSLN CAR-T cells, but not control CAR-T cells, exerted a significant lysis effect on $HEK293^{MSLN+}$ cells compared with control HEK293 cells (Fig. 3F and Fig. S1B).

Anti-MSLN CAR-T cells impede CDX tumor in vivo

To test the effect of anti-MSLNCAR-T cells in vivo, a CDX model derived from Ovcar3, Hela and Tov-21 g cells were constructed. The treatment groups of Ovcar3 were given a single tail intravenous injection of anti-MSLNCAR-T cells at various doses (1×10^7, H; 3×10^6, M; or 1×10^6, L; cells in 200 μL of PBS), and the control groups were treated with PBS or Mock CAR-T cells (Fig. 4A). Tumor volume was significantly inhibited in mice treated with anti-MSLN CAR-T cells but was not inhibited in mice treated with PBS or Mock CAR-T cells (Fig. 4B). No significant difference was observed in the body weight of mice between each group, except for the high-dose anti-MSLN CAR-T group (Fig. 4C). Before killing the mice, animal blood samples were collected to evaluate the toxicity of the CAR-T treatment on experimental animals via blood index analysis. The white blood cell (WBC) count, mean corpuscular hemoglobin concentration, and mean corpuscular volume in mice with tumor formation were significantly different from those in the original batch of tumor-free B-NDG mice. After CAR-T treatment, the WBC level of tumor-infected mice returned to normal, but other indicators were not significantly improved (Table. S2). After 23 days since the anti-MSLN CAR-T cell therapy, the tumors completely disappeared in the high- and medium-dose treatment groups, and only one small tumor mass was detected in the low-dose group at 42 days. On the contrary, Mock CAR-T cells and PBS did not reduce tumor burden in the control groups (Fig. 4D and Fig. S1C). In addition, 7 days after CAR-T cell injection, the serum cytokine (IL-2, TNF-α, and IFN-γ) levels were higher in the anti-MSLN CAR-T cells treatment groups than in the control groups (Fig. 4E). The infiltration of anti-MSLN CAR-T cells in the Ovcar3 CDX model was further verified via IHC staining (labeled by CD3) at the endpoint. More tumor cells in anti-MSLN CAR-T cell-treated mice were deformed and destroyed than in Mock CAR-T cell-treated mice, which showed an increase in T cell infiltration (Fig. 4F). Hematoxylin and eosin (H&E) staining showed that the parenchymal organ structure (including the heart, liver, spleen, lung, kidney, and brain) of the high-dose anti-MSLN CAR-T cells-treated mice were not damaged (Fig. S1D).

The treatment groups of Hela were given different percentages of total dose (5×10^6, H; 2.5×10^6, M; or 1×10^6, L; cells in 200 μL of PBS).by tail vein injection for three consecutive days (Fig. S2A). Tumor volume was significantly inhibited in mice treated with anti MSLN CAR-T cells but was not inhibited in mice treated with PBS or Mock CAR-T cells (Fig.S2B). And no significant difference was observed in the body weight of mice between each group (Fig.S2C). The tumor inhibitory rate of anti-MSLN CAR-T in low, medium and high dose groups was 50.40, 51.48 and 82.48%, respectively, on day 43 after treatment (Fig.S2D) More antitumor activities were also observed in Tov-21g cell in vivo and in vitro models (Fig.S3A-E).

These results indicate that our anti-MSLN CAR-T cells can eliminate $MSLN^+$ tumors, especially on ovarian cancer in vitro and in vivo.

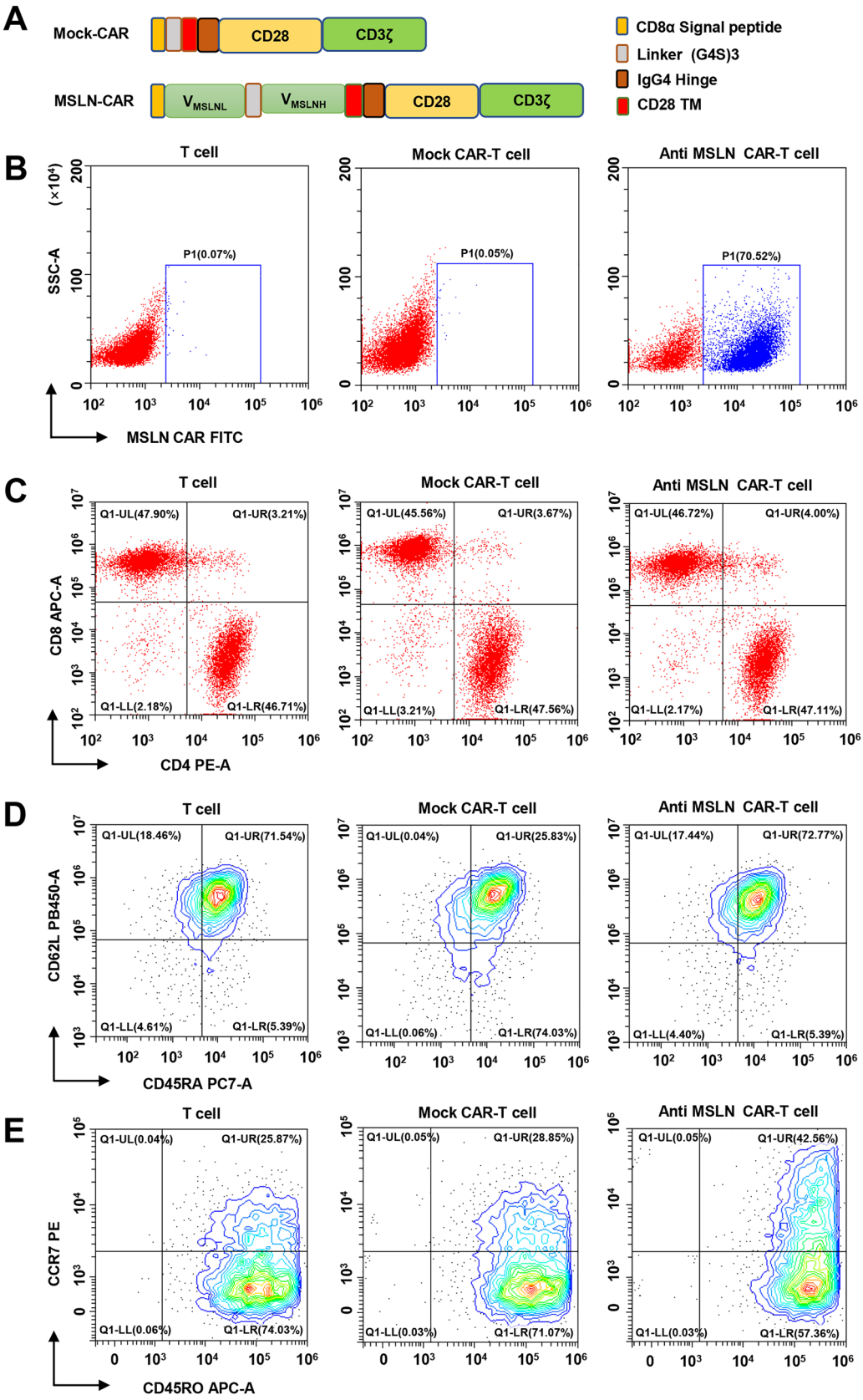
A
Mock-CAR
CD28
CD3ζ
MSLN-CAR
V MSLNL
V MSLNH
CD28
CD3ζ
CD8α Signal peptide
Linker (G4S)3
IgG4 Hinge
CD28 TM
B
T cell
Mock CAR-T cell
Anti MSLN CAR-T cell
SSC-A (×10⁴)
P1(0.07%)
P1(0.05%)
P1(70.52%)
MSLN CAR FITC
C
T cell
Mock CAR-T cell
Anti MSLN CAR-T cell
CD8 APC-A
Q1-UL(47.90%)
Q1-UR(3.21%)
Q1-LL(2.18%)
Q1-LR(46.71%)
Q1-UL(45.56%)
Q1-UR(3.67%)
Q1-LL(3.21%)
Q1-LR(47.56%)
Q1-UL(46.72%)
Q1-UR(4.00%)
Q1-LL(2.17%)
Q1-LR(47.11%)
CD4 PE-A
D
T cell
Mock CAR-T cell
Anti MSLN CAR-T cell
CD62L PB450-A
Q1-UL(18.46%)
Q1-UR(71.54%)
Q1-LL(4.61%)
Q1-LR(5.39%)
Q1-UL(0.04%)
Q1-UR(25.83%)
Q1-LL(0.06%)
Q1-LR(74.03%)
Q1-UL(17.44%)
Q1-UR(72.77%)
Q1-LL(4.40%)
Q1-LR(5.39%)
CD45RA PC7-A
E
T cell
Mock CAR-T cell
Anti MSLN CAR-T cell
CCR7 PE
Q1-UL(0.04%)
Q1-UR(25.87%)
Q1-LL(0.06%)
Q1-LR(74.03%)
Q1-UL(0.05%)
Q1-UR(28.85%)
Q1-LL(0.03%)
Q1-LR(71.07%)
Q1-UL(0.05%)
Q1-UR(42.56%)
Q1-LL(0.03%)
Q1-LR(57.36%)
CD45RO APC-A

◂**Fig. 2** Characterization of anti-MSLN CAR-T cells. **A** Schematic representation of retroviral CAR constructs of the humanized scFv (G11), linked to the CD8α Signal peptide, intracellular signaling domains CD28, (G4S)3 Linker, and CD3ζ in tandem. **B** Proportion of MSLN virus-infected isolated human T cells determined by flow cytometry. T cells and mock CAR-T cells served as controls. **C, D and E** Cell phenotype of anti-MSLN CAR-modified T cells was assessed by flow cytometry. Twelve days after lentivirus CAR transduction, the subsets and phenotype of T cell, Mock CAR-T and MSLN CAR-T cells were analyzed by FACS, including the expression of CD4, CD8, CD62L, CD45RA, CCR7 and CD45RO

Preclinical tissue crossover experiment based on G11-MSLN antibody

Before the clinical trial, a cross-reactivity test was conducted on the positive tissues with a high expression of MSLN and biotin-labeled G11 to distinguish between target organs bound "on-target" and nontarget organs bound "off-target" as well as to evaluate G11 toxicity. IHC revealed that the MSLN-positive tissues were significantly stained by biotin-labeled G11 at 2 or 20 μg/mL but not by control Biotin-Human IgG1 (Fig. S4). Then, the specific binding of Biotin-G11 to 11 kinds of tissues (performed in triplicate) originating from three different donors (donation from Nanjing First Hospital) was evaluated via IHC. Compared with the negative control group, the Biotin-G11 20 μg/mL group had specific reactions with eight tissues (incidence rate, 1/3–3/3), namely, the thymus, heart, lungs, kidney, fallopian tube, uterus, placenta, and skin (Table S3). Lower concentration of Biotin-G11 (2 μg/mL) only specifically reacted with five tissues, namely, lung, fallopian tube, uterus, placenta, and skin. These data provide references for animal experiments, suggesting possible toxic reactions, and provide a reference for future clinical safe drug use in humans.

Patient characteristics

Three patients with chemotherapy–refractory metastatic ovarian cancer received anti-MSLN CAR-T cells immunotherapy for several months. The hospital pathology department performed IHC staining and found that patient tumors were positive for MSLN: patient 001 had a staining intensity score of 2 + , and the other two patients had staining intensity scores of 1 + (Fig. S5A; see Table 1 for patient baseline data). No patient had achieved even partial response (PR) with the most recent chemotherapy-containing salvage regimen before joining the anti-MSLN CAR-T therapy regimen. In this study, the patients administrated multiple planned anti-MSLN CAR-T cell infusions, and their malignant tumor responses were regularly assessed.

Preparation of anti-MSLN CAR-T cells using PBMCs of patients

Anti-MSLN CAR-T cells were prepared by using PBMCs from these three severely affected patients and tested the killing effect of CAR-T cells from two patients on cancer cell lines in vitro (Fig. S5B). Microscopic examination revealed that the MSLN CAR-T cells produced using the patients' PBMC had a significant killing effect on the target cells that expressed MSLN. Cell CAR expression was measured via flow cytometry 1 to 3 days before each infusion. About 70% (range, 58.04–83.04%) of infused T cells expressed anti-MSLN CAR (Fig. S6), negative mycoplasma, negative bacterial and fungal cultures.

Patients with advanced ovarian cancer experience remission with anti-MSLN CAR-T immunotherapy

Based on the preclinical results, we conducted an investigator-Initiated clinical study on advanced ovarian carcinoma patients with MSLN expression to further explore the clinical safety and feasibility of the anti-MSLN CAR-T cells therapy. The clinical trial design is described in Fig. 5A. Three patients were enrolled based on the patient inclusion and exclusion criteria and received anti-MSLN CAR-T cells therapy. The dose per infusion is presented in Table S4. The anti-MSLN CAR-T cells therapy was tolerable in patients who had low tumor burdens and were in good clinical condition, even for doses reached to 3×10^7 CAR-positive cells. As shown in Table. 2 and Table S1, chemotherapy-related myelosuppression was observed in two patients, determined by the investigators to be unrelated to our study drug, and one patient had asymptomatic increases in serum Crea after multiple dosing. And no greater than grade 2 neurotoxicity and CAR-T-related infusion reactions were observed in any patients.

We next evaluated the antitumor activity of MSLN CAR-T from three patients. Two patients were alive at the time of data analysis, and three patients were assessed by stages according to the standard RECIST (Version 1.1) (Fig. 5B). For patient 001, after the first infusion of CAR-T cells, tumor lesions were significantly reduced (by 23%) despite the patient not achieving PR. Unfortunately, the patient suddenly died due to an unknown cause 200 days after CAR-T cell infusion. For patient 002, within 8 months after anti-MSLN CAR-T cells reinfusion, metastases did not decrease, and overall tumor lesions did not develop. The patient did not suffer any toxic effects and was evaluated by stage stable disease (SD). For patient 003, incomplete data showed that after the infusion of CAR-T cells, the overall volume of the tumor increased by 30% compared with that of the baseline tumor. Representative images from CT scans used to monitor metastatic lesions are presented in Fig. 5D.

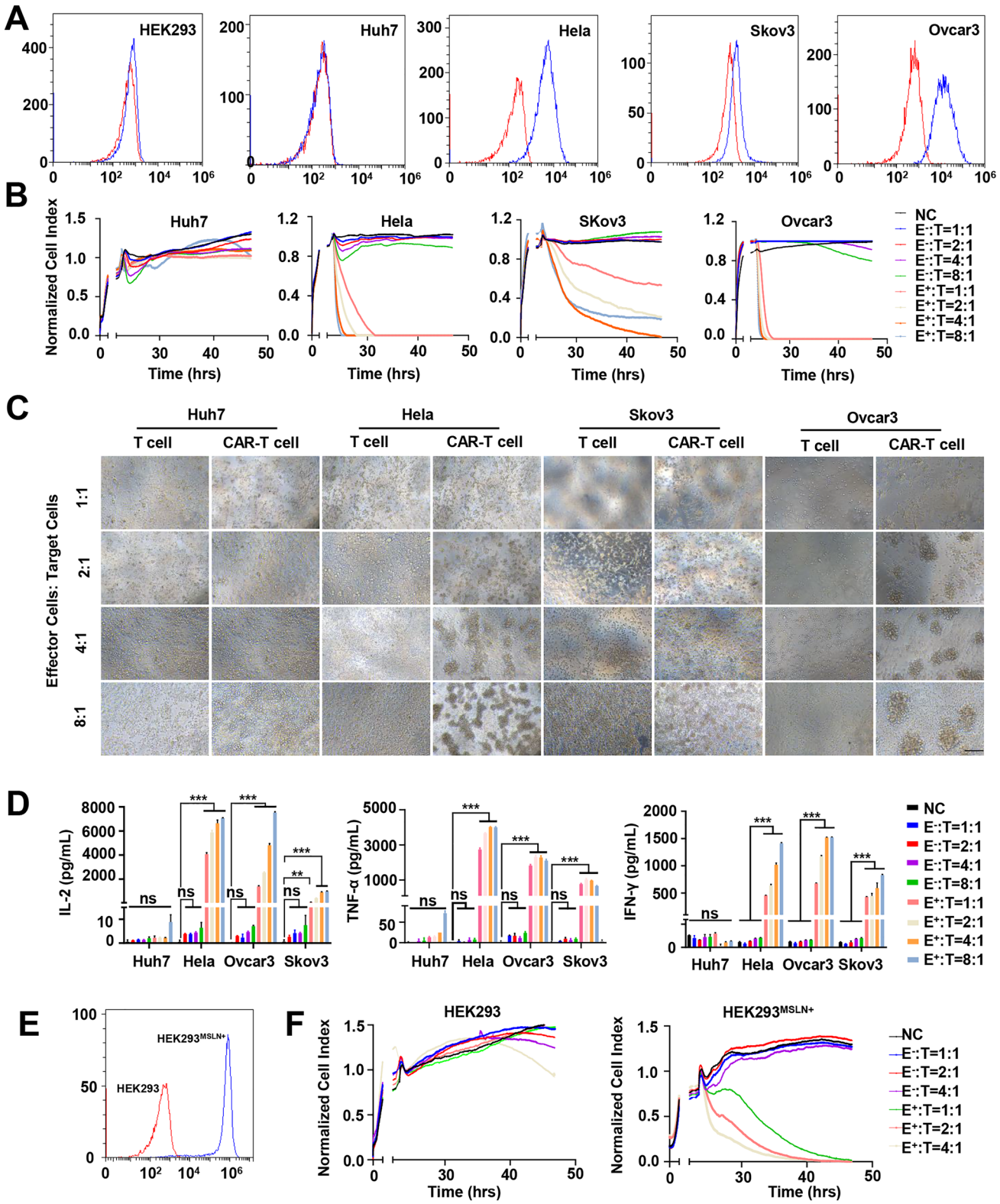

We monitored the serum CA12-5 levels throughout the studies. Patients who had clinically meaningful antitumor activity of progressive disease or SD had high-percentage reductions in the serum CA12-5 levels after anti-MSLN CAR-T cells infusion (Fig. 5D).

To evaluate the pharmacokinetic characteristics of MSLN-CAR-T cells, the anti-MSLN CAR copy numbers

◂**Fig. 3** Tumor cells elimination capacity in vitro. **A** Detection of MSLN expression in five human cell lines, including HEK293, Huh7, Hela, Skov3 and Ovcar-3 cells by flow cytometry. Cells were incubated with anti-MSLN antibody (blue) or its corresponding isotype control (red). Same below. **B** A real-time cytotoxicity assay (xCELLigence RTCA SP) was used to evaluate the lysis of the indicated tumor cells. Tumor cells treated with mock CAR-T (E^-) cells or MSLN CAR-T (E^+) cells at the indicated E/T ratios over a 50-h period. The NC group did not add other cells to co-incubate as a control. Same below. **C** Lysis of spheres of target ovarian cancer cell cultures in the presence of anti-MSLN CAR-T cells at different effector: target ratios (E: T). (Scale bar: 200 μm). **D** The release of cytokines of tumor cells after co-cultivation with anti-MSLN CAR-T cells. ($n=3$) **E** Lentivirus-mediated MSLN overexpression in HEK293 cell line by flow cytometry. **F** The real-time cytotoxicity assay is used to evaluate the lysis of MSLN CAR-T on HEK293 $^{MSLN+}$ cells. mean ± SD; two-way ANOVA, $^{***}P<0.001$, $^{****}P<0.0001$

were monitored weekly in the first month after infusion and monthly thereafter (Fig. 6A). These CAR copy numbers in the peripheral blood of patient 001 rapidly increased within 1 week after each reinfusion and lasted longer than 36 days according to the monitoring conducted in the later period of the study. The symptoms of intestinal obstruction were relieved after the first two infusions and disappeared after the third. For patient 002, the CAR-T cell DNA copy number peaked at 4 days after MSLN cell infusion and remained above the baseline for more than 3 weeks. For patient 003, a significant increase in DNA copy number was observed only after the second reinfusion of CAR-T cells.

A large number of cytokines can recruit and activate more immune cells and cause a wider range of anti-tumor immune effects, but there are also hidden dangers of causing cytokine release syndrome. CRS is a major clinical concern for patients receiving CAR-T cell therapy. We monitored the patients' cytokine serum levels and body temperatures during the study period (Fig. 6C and Fig. 6D). All patients experienced grade 1 fever. The anti-MSLN CAR-T cells produced cytokines in a MSLN-specific manner. For patients 001 and 002, the IL6 levels peaked at 105.89 and 189.01 pg/mL, respectively, at the same time that their body temperature increased. Three subjects experienced low-grade CRS (grade 1). This is consistent with the CRS clinical observation results of other patients who received anti-MSLN CAR-T cells infusion. We did not see the occurrence of clinical adverse reaction symptoms such as nausea, vomiting, diarrhea, asthenia, asthenia and headache that can be judged as DLT.

Discussion

Ovarian cancer is one of the most lethal gynecologic malignancies among women, with a 5-year patient survival of not more than 30% [24]. Although targeted therapy has improved the prognosis of ovarian cancer patients, the 5-year survival rate for most ovarian cancer patients is still unsatisfactory [25]. Therefore, there is an urgent need to formulate targeted strategies to improve the clinical outcome of patients with ovarian cancer and prolong their survival.

The applications of CAR-T cells have achieved remarkable success in hematologic malignancies. Two CAR-T products approved by the US FDA for the treatment of acute lymphocytic leukemia have demonstrated the potential clinical application of this therapy [26, 27]. Despite tremendous progress in the development and availability of CAR-T cell therapy, ovarian cancer remains largely incurable, and patients in relapse or with refractory disease have a poor prognosis. CAR-T cells have exhibited dramatic efficacy in a small number of patients with ovarian cancer, whereas several patients are still in remission after infusion [28]. To generate more effective CAR-T cells, it is crucial to select appropriate antigens to kill tumor cells with minimum toxicity. We selected MSLN as the target for our second-generation CAR structure owing to its high expression in ovarian cancer [29].

Barriers to effective CAR-T cell therapy in the clinic include immunogenicity of murine CAR-T, severe toxicities, immunosuppression in the tumor microenvironment, limited antitumor activity, antigen escape, restricted trafficking, poor persistence, and migration [30]. CARs are designed to enable T cells to have the ability to target specific proteins, and their single-chain antibody component allows CAR-T to specifically recognize tumor cell surface antigens [31]. Biotherapeutic molecules with nonhuman sequences can cause immune responses. The majority of CARs used in clinical trials are mouse-derived, which can lead to humoral and $CD8^+$ T cell-mediated immune responses resulting in immune rejection [32]. Reintroduction of CAR-T cells containing a mouse component into patients who develop $CD19^+$ relapse following initial treatment is largely ineffective [33]. In addition, clusters of mouse CAR receptors on the cell surface can generate tonic signals that lead to T cell depletion. In 2016, CAR-T with humanized scFv entered clinical trials, and humanized CARs exhibited similar cytotoxic activity to mouse CARs but with enhanced persistence due to lower immunogenicity [6]. For example, affinity is a particularly important antigen-binding domain parameter as it determines CAR function[30]. To recognize antigens on tumor cells, induce CAR signaling, and activate T cells, the CAR's antigen-binding affinity must be sufficiently high but not high enough to result in activation-induced death of the CAR-expressing T cell or to trigger toxicities [34]. A new study shows that low-affinity CAR T cells exhibit reduced phagocytosis, prevent rapid antigen loss, and increase CAR T cell expansion[35]. Therefore, deciding which humanized antibody domain to use is critical when developing effective CAR-T cell therapy.

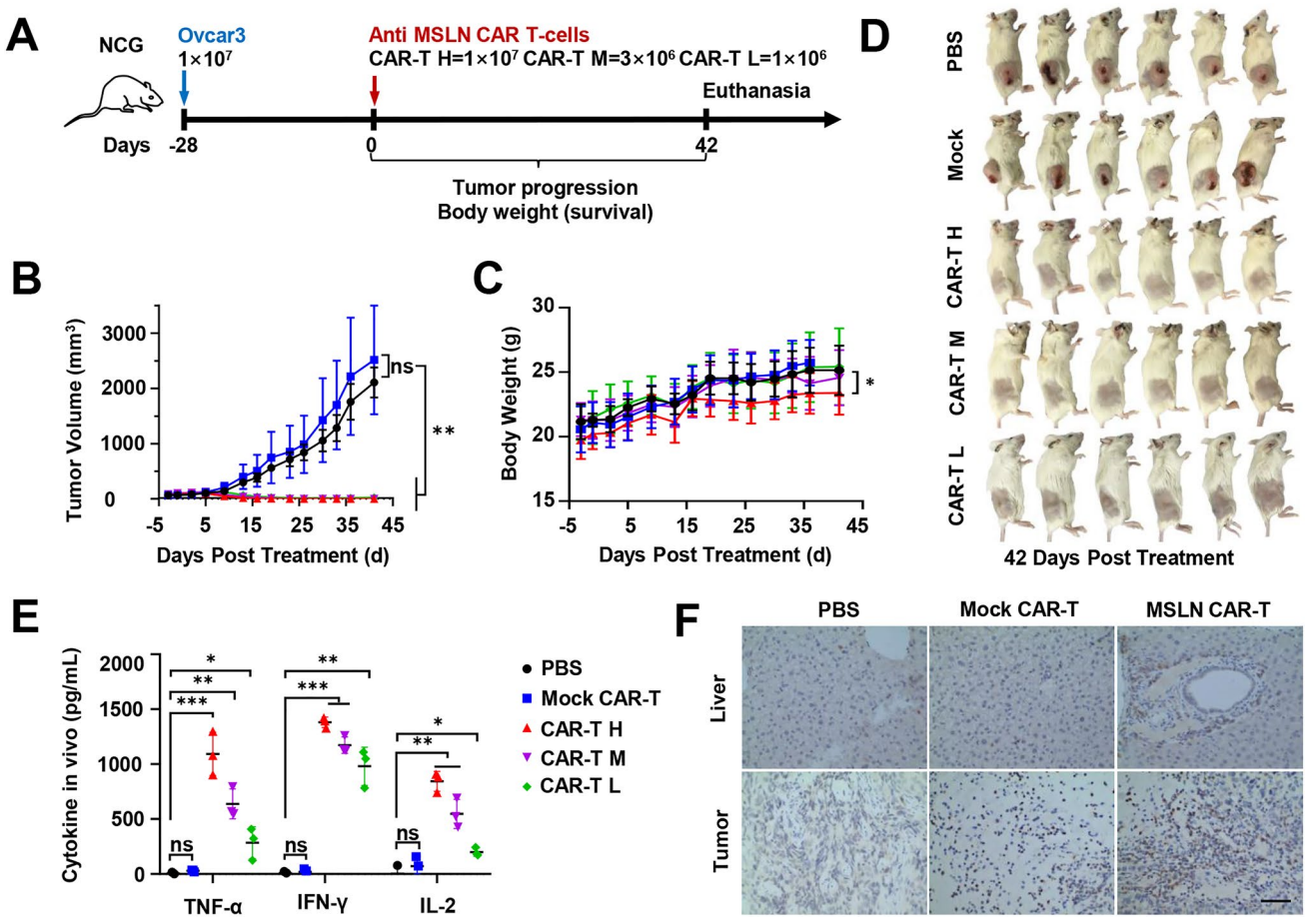

Fig. 4 Specific tumor elimination capacity of anti-MSLN CAR-T cells in vivo in an i.v. NDG model. **A** Schematic representation of the experiments. CAR-T H: MSLN CA-T high dose. CAR-T M: MSLN CA-T middle dose. CAR-T L: MSLN CA-T low dose. **B** Tumor volumes were plotted versus time for each group. ($n=6$). **C** The body weight of NDG mice was measured before tumor formation and CAR-T cell injection, and continuously measured every 3–4 days after CAR-T cell injection. The line represents the mean ± SD. ($n=6$) **D** Pictures of mice sacrificed at the end of the experiment. The tumor volume grew to 2000 cm^3, and the mice of each group were sacrificed and photographed. **E** ELISA results showed the IL-2, TNF-α and IFN-γ secretion levels in mice blood treated by PBS, Mock CAR-T different doses of anti-MSLN CAR-T cells. **F** The expression of CD3 in mouse liver and tumor tissues after Mock CAR-T and MSLN-L CAR-T cells treatment. Representative immunostaining images of MSLN CAR T cells infiltration in mice tumor tissues ($n=5$). Scale bars, 50 mm. Mean ± SD; two-way ANOVA, $^{***}P<0.001$, $^{****}P<0.0001$

Table 1 Patients baseline data

Patient No	Age (at infusion in years)	Sex	Weight (kg)	Malignancy	No. of Prior Therapies	Staging of ovarian cancer
001	59	Female	61	Serous Papillary Cystadenoma of Ovary	3	IV
002	66	Female	47	Endometrioid carcinoma of the ovary	5	IV
003	57	Female	65	Bilateral ovarian adenocarcinoma	3	IV

All prior diagnoses and therapies for each patient are listed in Data Supplement

In the present study, we screened anti-MSLN antibodies through a scFv phage-displayed library designed to contain the heavy- and light-chain fusion variable regions encoded by human antibody genes. The isolated phage clones with MSLN protein affinity were assessed for their cancer-cell-targeting and cancer-cell-growth -suppressing potential. Considerable improvement has been made to CAR signaling domains. Then, we used the antibodies

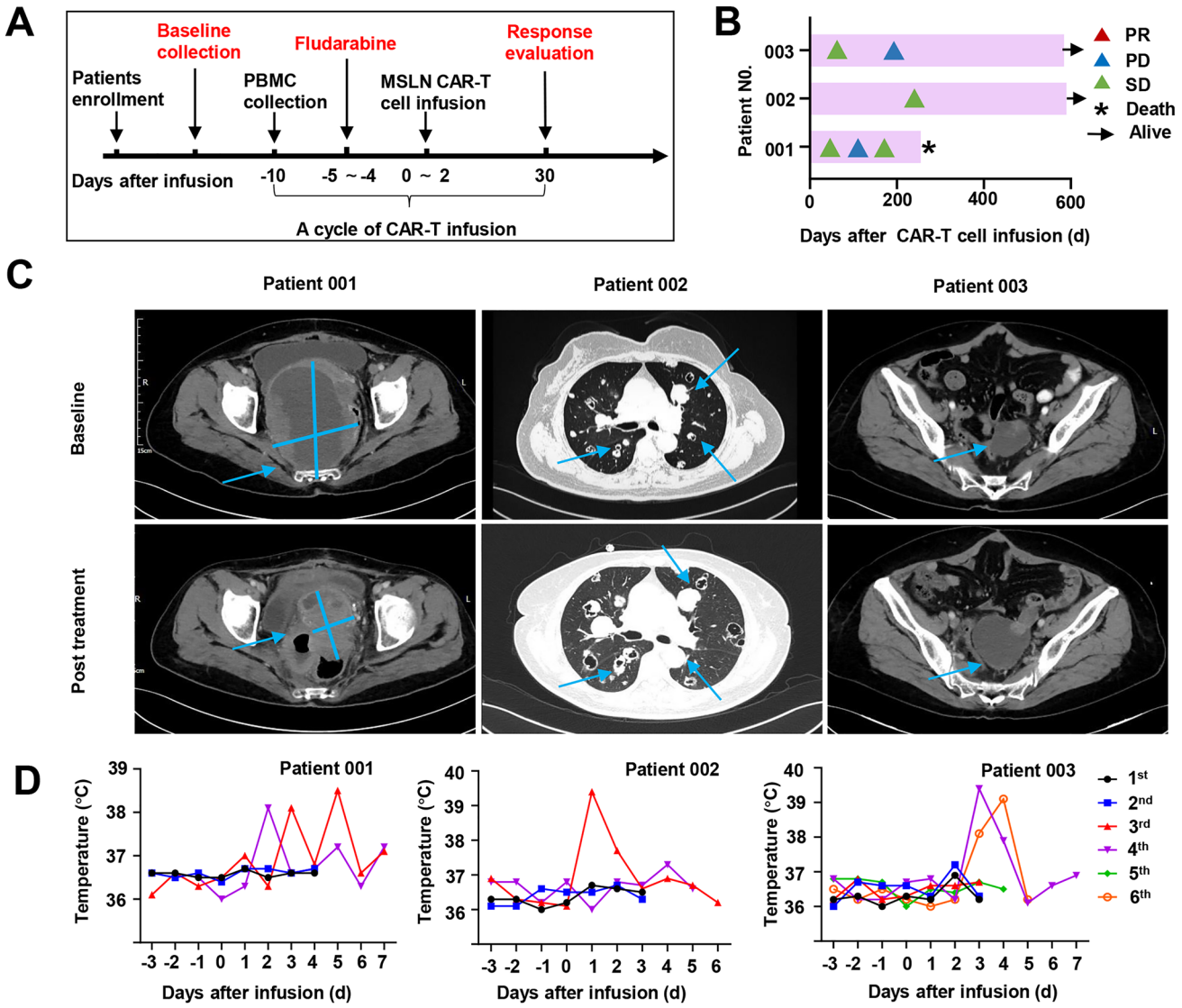

Fig. 5 Clinical response. **A** The scheme of anti-MSLN CAR-T cell treatment. According to the patient's status, patient 001 was pretreated with Fudarabine before CAR-T cell reinfusion and underwent 4 times reinfusions. Patient 002 and 003 were reinfused with CART cells 6 times and 4 times, but due to poor physical condition, lymphatic clearance was not performed before CAR-T reinfusion. **B** Swimmer plot Shows the patient's disease remission at various stages of treatment. **C** Representative CT images of patients before and after CAR-T treatment. The solid blue lines indicate the long and short diameters of the tumor. The blue arrows mark the location of the tumor and lymph nodes. **D** Daily patient body temperature distribution chart. Changes in patient body temperature before and after reinfusion were monitored. Fever without patients requiring pharmacological intervention

humanized with different affinities for MSLN, respectively, to construct CAR-T cells. Humanized anti-MSLN CAR-T cells were evaluated for their tumor-killing ability on MSLN-positive cancer cell lines in vitro. We found that CAR-T cells synthesized by the G11-MSLN sequence had strong killing effect and dose-dependent antitumor activity. Subsequently, we evaluated the antitumor ability of humanized anti-MSLN CAR-T cells on B-NDG mouse models of ovarian cancer. Our results indicate that MSLN CAR-T induced significant cytokine release, which led to complete tumor regression in vivo.

A phase I clinical trial[36] evaluated the safety and efficacy of aPD1-MSLN-CAR-T in subjects with MSLN-positive advanced solid tumors who had failed standard therapy. The doses of CAR-T cells were 5×10^6/kg, 5×10^7/kg and 1×10^8/kg, respectively, and subjects received preconditioning for 3 consecutive days fludarabine and Cyclophosphamide before cell infusion. The survival time (PFS) of 10 subjects was 97 days. The adverse events were mild fatigue and fever, abdominal pain in 1 (10%) patient, cytokine release syndrome (both grades 1 and 2) observed in 10 (100%) patients. Another phase I clinical trial[37] evaluated

Table 2 Blood biochemical monitoring after the CAR-T cell reinfusion

Patient ID	Date	TC (2.8–6) mmol/L	ALB(35–55) g/L	AST (0–45) U/L	GLU (3.9–6.1) mmol/L	GGT(0–73) U/L	TP(55–85) g/L	TBIL (0–20.5) μmol/L	TG(0.56–1.7) mmol/L	ALP (45–129) U/L	CREA(44–97) μmol/L	ALT(10–49) U/L
001	39	–	42.4	25	6.6	61	68.7	6.7	–	188	83	20
	46	4.30	49.5	25	–	54	80.7	6.0	2.01	169	91	15
	123	3.79	41.6	18	9.4	44	41.6	7.9	1.69	154	111	10
	144	2.73	30.4	29	5.9	71	55.3	9.9	0.95	137	160	16
	149	3.48	33.8	8	13	51	61.6	9.9	2.32	94	135	6
	249	–	40.3	16	3.4	42	68.5	5.1	–	161	436	11
	258	–	35.4	17	7.5	46	60.7	4.4	–	157	514	10
002	1	–	38.1	10	16.8	17	63	7.2	–	52	55	9
	3	–	40.6	9	19.5	19	64.5	4.9	–	55	58	9
	12	5.91	42.9	14	11.6	17	99.2	7.8	1.85	57	56	8
	21	5.09	41.6	14	7.9	17	65.6	8.3	1.55	51	57	8
	27	–	45.1	11	21	21	71.1	5.9	–	61	60	7
	31	–	66.3	10	16	18	66.3	9.6	–	57	49	5
	48	6.30	40.4	11	12.8	15	67.1	6.2	1.65	56	63	7
	57	5.87	37.7	10	14.2	18	61.7	6.4	1.70	58	62	5
	62	–	42.9	9	16.1	17	70.6	5.4	–	58	53	9
	66	–	43	11	16.4	18	70.4	8.3	–	54	60	8
	79	4.73	38.1	9	9.8	17	63.2	3.3	1.74	60	55	6
	90	4.87	40.3	11	11.5	19	67.8	4.0	1.91	54	52	7
	96	5.64	40.6	11	11.1	18	65.1	5.2	1.76	50	60	9
	101	–	43.1	12	15.7	17	69	7.3	–	47	55	10
003	− 2	5.82	45.8	31	5.5	199	71.4	6.8	2.17	119	65	44
	3		43.4	38	5.1	181	69.8	6.3	–	126	58	44
	9	5.52	48	31	5.4	159	78.2	7.6	1.71	102	63	38
	27	5.20		27	5.2	105	73.3	7.4	2.47	94	63	33
	31	5.19	44.4	34	4.9	119	70.7	7.2	2.77	96	61	42
	63	24	48	24	7.5	200	77.2	8.6	1.27	171	67	32
	77	4.19	39.5	22	5.3	74	64.4	7.2	1.53	98	62	24
	87	4.78	42	24	5.4	53	–	5.1	1.59	27	63	19
	93	4.22	40.0	25	5.3	62	65.7	5.6	1.59	99	58	22
	100	4.65	44.4	23	6.0	60	74.4	6.8	2.24	112	64	20

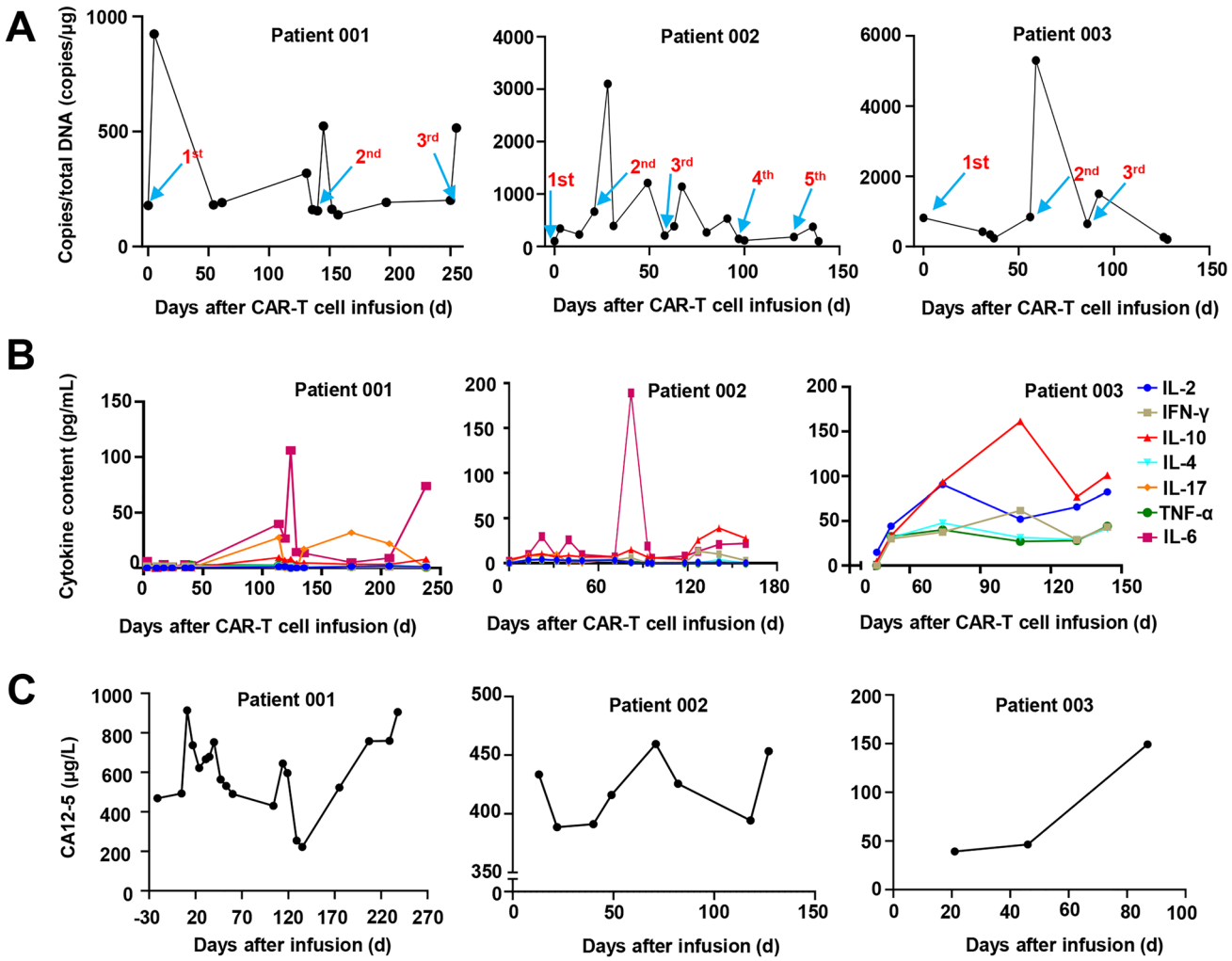

Fig. 6 Expansion of CAR-T cells and levels of CA125 and cytokines during treatment. **A** Detection of MSLN-CAR-T in blood during immunotherapy. Anti-MSLN CAR-T expansion and persistence in the peripheral blood was detected by qPCR. Blue arrows indicate the time points of each reinfusion of CAR-T cells. **B** Cytokine dynamics after sevaral CAR-T infusions. Concentrations of IL-2, 4, 6, tumor necrosis factor (TNF-α) and interferon (IFN-γ), etc. were measured by flow cytometry. **C** Detection of plasma CA125 levels in hospital medical laboratory. The curve starts from the day first time infusion CAR-T cells

the safety, efficacy and PK of lentiviral-transfected MSLN-specific CAR-T (Lenti-CART-Meso) cells in subjects with advanced solid tumors who had failed chemotherapy feature. The proliferation and survival time of Lenti-CART-Meso cells in peripheral blood were detected by qPCR before and after infusion. The PK results showed that the number of Lenti-CART-Meso cells in the peripheral blood of subjects reached a peak at about 6 to 14 days, and then the level of Lenti-CART-Meso cells decreased significantly. At the second month, 15 subjects were Lenti-CART-Meso cells were not detected in 9 cases. In our clinical trials, three patients with mesothelioma were treated in a clinical trial of MSLN-CAR-T treatment and retrospectively evaluated for antitumor response and OS. The MSLN CAR-T produced from G11 sequences also showed strong antitumor activity and low toxicity.

The two main safety concerns associated with the use of CAR-T treatment are the neurotoxicity and cytokine storms associated with immune responses. Our current three-case preliminary clinical study demonstrated that there was no grade 2–4 adverse events or major complications in our study; one patient achieved CR and two patients achieved SD. Taken together, our data indicate that MSLN CAR-T cell therapy would provide a promising immunotherapeutic approach for advanced ovarian cancer. The limitations of the study are the more patients are needed to validate the clinical responses observed in the current case. Thus, based on the safety and effectiveness test results in this study, we are preparing to conduct a formal phase I clinical trial.

Conclusions

In summary, our findings confirm that our second-generation anti MSLN CAR-T cells targeting MSLN showed effective anti-tumor effect on MSLN-positive cancer cells in vitro and in vivo. The preliminary clinical data demonstrated that our anti-MSLN CAR-T cells may exert potent antitumor activities in patients with ovarian cancer. These data suggest a potential value of using anti-MSLN CAR-T to treat ovarian cancer patients in the clinic. Our study implicated an effective strategy in the treatment of ovarian cancer by using anti-MSLN CAR-T immunotherapy to provide alleviation from tumor and hopefully prolong patient life.

Supplementary Information The online version contains supplementary material available at https://doi.org/10.1007/s00262-022-03238-w.

Acknowledgements This study was supported by the National Natural Science Foundation of China (81872284) and the Priority Academic Program Development of Jiangsu Higher Education Institutions. We thank every member of the laboratory, as well as the patients and their families, and Nanjing Blue Shield Co. Thanks also to Junfeng Zhang, Liang Jing and Yaoyao Zhao from Nanjing Blue Shield Co. for technical support.

Author contributions JC, ZG and ZH contributed to the conception and design; JC, JH, LG, FJ, JL, ZC, LJ, YZ^2, RS, LM, SJ, YZ^4, QZ, JL and SY contributed to the acquisition of data; JC, JH, FJ, LJ, JL, MZ and FZ contributed to the analysis and interpretation of data; JC, LG and FJ contributed to the writing, review, and/or revision of the manuscript; JH, LJ, RS, LM, YZ^2, SJ, YZ^4, QZ, JL and SY collected the data of clinical characteristics; JC, JH, YZ, LJ, LG, FJ, JL, SJ, YZ, QZ, SY, ZG and ZH contributed to the administrative, technical, or material support; ZG and ZH supervised the study.

Data availability The authors declare that all data supporting the results in this study are available within the paper and its supplementary information. Source data for the figures in this study are available from the corresponding author upon reasonable request.

Declarations

Conflict of interest The authors declare no conflict of interests.

Ethical approval and consent to participate All in vivo animal experiments were approved by the Committee on the Ethics of Animal Experiments of Nanjing Normal University (IRB#2020–0047). The clinical experiment was approved by the Experimental Ethics Committee of the Eastern Theater General Hospital (formerly the 81st Hospital of the People's Liberation Army) (81YY-KYLL-04–25-02).

References

1. Siegel RL, Miller KD, Fuchs HE, Jemal A (2021) Cancer statistics, 2021. CA: A Cancer J Clin 71:7–33. https://doi.org/10.3322/caac.21654
2. Sung H, Ferlay J, Siegel RL, Laversanne M, Soerjomataram I, Jemal A, Bray F (2021) Global cancer statistics 2020: globocan estimates of incidence and mortality worldwide for 36 cancers in 185 countries. CA: A Cancer J Clin 71:209–49. https://doi.org/10.3322/caac.21660
3. Matulonis UA, Sood AK, Fallowfield L, Howitt BE, Sehouli J, Karlan BY (2016) Ovarian cancer. Nat Rev Dis Primers 2:16061. https://doi.org/10.1038/nrdp.2016.61
4. Tyagi K, Mandal S, Roy A (2021) Recent advancements in therapeutic targeting of the warburg effect in refractory ovarian cancer: a promise towards disease remission. Biochim et Biophys Acta (BBA) - Rev on Cancer 1876(1):188563. https://doi.org/10.1016/j.bbcan.2021.188563
5. Lheureux S, Gourley C, Vergote I, Oza AM (2019) Epithelial ovarian cancer. The Lancet 393:1240–1253. https://doi.org/10.1016/S0140-6736(18)32552-2
6. Jiang C, Gang W, Hai C et al (2018) Potent anti-leukemia activities of humanized cd19-targeted chimeric antigen receptor t (car-t) cells in patients with relapsed/refractory acute lymphoblastic leukemia. Am J Hematol 93:851–858. https://doi.org/10.1002/ajh.25108
7. Upadhaya S, Yu XA, Shah M, Correa D, Campbell JR (2021) The clinical pipeline for cancer cell therapies. Nat Rev Drug Discov 20(7):503–504. https://doi.org/10.1038/d41573-021-00100-z
8. Choi T, Kang Y (2021) Chimeric antigen receptor (car) t-cell therapy for multiple myeloma. Pharmacol Therapeut. https://doi.org/10.1016/j.pharmthera.2021.108007
9. Ji F, Zhang F, Zhang M et al (2021) Targeting the dna damage response enhances cd70 car-t cell therapy for renal carcinoma by activating the cgas-sting pathway. J Hematol Oncol 14:152. https://doi.org/10.1186/s13045-021-01168-1
10. Tian Y, Li Y, Shao Y, Zhang Y (2020) Gene modification strategies for next-generation car t cells against solid cancers. J Hematol Oncol. https://doi.org/10.1186/s13045-020-00890-6
11. Andrea AE, Chiron A, Bessoles S, Hacein-Bey-Abina S (2020) Engineering next-generation car-t cells for better toxicity management. Int J Mol Sci 21:8620. https://doi.org/10.3390/ijms21228620
12. Cappell KM, Kochenderfer JN (2021) A comparison of chimeric antigen receptors containing cd28 versus 4–1bb costimulatory domains. Nat Rev Clin Oncol 18:715–727. https://doi.org/10.1038/s41571-021-00530-z
13. Mullard A (2017) Fda approves first car t therapy. Nat Rev Drug Discov 16:669. https://doi.org/10.1038/nrd.2017.196
14. Crees ZD, Ghobadi A (2021) Cellular therapy updates in b-cell lymphoma: the state of the car-t. Cancers 13:5181. https://doi.org/10.3390/cancers13205181
15. Neelapu SS, Jacobson CA, Oluwole OO et al (2020) Outcomes of older patients in zuma-1, a pivotal study of axicabtagene ciloleucel in refractory large b-cell lymphoma. Blood 135:2106–2109. https://doi.org/10.1182/blood.2019004162
16. Schoutrop E, El-Serafi I, Poiret T et al (2021) Mesothelin-specific car t cells target ovarian cancer. Cancer Res 81:3022–3035. https://doi.org/10.1158/0008-5472.CAN-20-2701
17. Zhang Q, Liu G, Liu J et al (2021) The antitumor capacity of mesothelin-car-t cells in targeting solid tumors in mice. Mol Ther - Oncolytics 20:556–568. https://doi.org/10.1016/j.omto.2021.02.013
18. Lv J, Li P (2019) Mesothelin as a biomarker for targeted therapy. Biomark Res. https://doi.org/10.1186/s40364-019-0169-8
19. Hassan R, Thomas A, Alewine C, Le DT, Jaffee EM, Pastan I (2016) Mesothelin immunotherapy for cancer: ready for prime time? J Clin Oncol 34:4171–4179. https://doi.org/10.1200/JCO.2016.68.3672
20. Beatty GL, Hara O, M H, Lacey S F, et al (2018) Activity of mesothelin-specific chimeric antigen receptor t cells against pancreatic carcinoma metastases in a phase 1 trial. Gastroenterology 155:29–32. https://doi.org/10.1053/j.gastro.2018.03.029

21. Zhao R, Cui Y, Zheng Y et al (2021) Human hyaluronidase ph20 potentiates the antitumor activities of mesothelin-specific car-t cells against gastric cancer. Front Immunol 12:660488. https://doi.org/10.3389/fimmu.2021.660488
22. Klampatsa A, Dimou V, Albelda SM (2021) Mesothelin-targeted car-t cell therapy for solid tumors. Expert Opin Biol Th 21:473–486. https://doi.org/10.1080/14712598.2021.1843628
23. Molloy ME, Austin RJ, Lemon BD et al (2021) Preclinical characterization of hpn536, a trispecific, t-cell–activating protein construct for the treatment of mesothelin-expressing solid tumors. Clin Cancer Res 27:1452–1462. https://doi.org/10.1158/1078-0432.CCR-20-3392
24. Wu S, Wang J, Sun J, He Z, Zhang W, Zhou J (2019) Real-world impact of survival by period of diagnosis in epithelial ovarian cancer between 1990 and 2014. Front Oncol 9:639. https://doi.org/10.3389/fonc.2019.00639
25. Atallah GA, Abd.Aziz NH, Teik CK, Shafiee MN, Kampan NC (2021) New predictive biomarkers for ovarian cancer. Diagnostics 11:465. https://doi.org/10.3390/diagnostics11030465
26. Wang Z, Guo Y, Han W (2017) Current status and perspectives of chimeric antigen receptor modified t cells for cancer treatment. Protein Cell 8:896–925. https://doi.org/10.1007/s13238-017-0400-z
27. Podar K, Leleu X (2021) Relapsed/refractory multiple myeloma in 2020/2021 and beyond. Cancers 13:5154. https://doi.org/10.3390/cancers13205154
28. Rodriguez-Garcia A, Sharma P, Poussin M et al (2020) Car t cells targeting misiir for the treatment of ovarian cancer and other gynecologic malignancies. Mol Ther 28:548–560. https://doi.org/10.1016/j.ymthe.2019.11.028
29. Morello A, Sadelain M, Adusumilli PS (2016) Mesothelin-targeted cars: driving t cells to solid tumors. Cancer Discov 6:133–146. https://doi.org/10.1158/2159-8290.CD-15-0583
30. Sterner RC, Sterner RM (2021) Car-t cell therapy: current limitations and potential strategies. Blood Cancer J 11:69. https://doi.org/10.1038/s41408-021-00459-7
31. Li W, Song X, Jin Y, Li F, Yu H, Cao C, Jiang Q (2017) Carts for solid tumors: feasible or infeasible? Oncol Res Treat 40:540–546. https://doi.org/10.1159/000477095
32. DeRenzo C, Gottschalk S (2019) Genetic modification strategies to enhance car t cell persistence for patients with solid tumors. Front Immunol 10:218. https://doi.org/10.3389/fimmu.2019.00218
33. Berger C, Flowers ME, Warren EH, Riddell SR (2006) Analysis of transgene-specific immune responses that limit the in vivo persistence of adoptively transferred hsv-tk–modified donor t cells after allogeneic hematopoietic cell transplantation. Blood 107:2294–2302. https://doi.org/10.1182/blood-2005-08-3503
34. Krishna M, Nadler SG (2016) Immunogenicity to biotherapeutics – the role of anti-drug immune complexes. Front Immunol 7:21. https://doi.org/10.3389/fimmu.2016.00021
35. Ml O, Erv M, Sv R, Jd B, Ap R, Al W, Da TL (2022) Low-affinity car t cells exhibit reduced trogocytosis, preventing rapid antigen loss, and increasing car t cell expansion. Leukemia. https://doi.org/10.1038/s41375-022-01585-2
36. Fang J, Sun Y, Guo X et al (2020) Safety and efficacy of chimeric antigen receptor t cells modified to target mesothelin and express pd-1 antibodies in patients with relapsed/refractory solid cancers in a phase i trial. J Clin Oncol 38:3039. https://doi.org/10.1200/JCO.2020.38.15_suppl.3039
37. Haas AR, Tanyi JL, O'Hara MH et al (2019) Phase i study of lentiviral-transduced chimeric antigen receptor-modified t cells recognizing mesothelin in advanced solid cancers. Mol Ther 27:1919–29. https://doi.org/10.1016/j.ymthe.2019.07.015